Available online at www.sciencedirect.com
SCIENCE DIRECT®
PERGAMON
Minerals Engineering 15 (2002) 795–808
MINERALS ENGINEERING
This article is also available online at: www.elsevier.com/locate/mineng

The adaptation of *Thiobacillus ferrooxidans* for the treatment of nickel–iron sulphide concentrates ☆

L.J. Mason, N.M. Rice *

Department of Mining and Mineral Engineering, School of Process, Environmental and Materials Engineering, University of Leeds, Leeds LS2 9JT, West Yorkshire, UK

Received 2 May 2002; accepted 4 June 2002

Abstract

Thiobacillus ferrooxidans was successfully adapted to copper–nickel–iron and pyrrhotite concentrates. Bacterial leaching in a culture medium at initial pH 2 resulted in increased solubilisation of the metals for both concentrates. Two strains, designated *NatTf* and *ConTf*, both showed similar overall % metal solubilisation in the order Ni > Fe > Cu. Extraction corresponded to the growth phase but the leaching rate for *ConTf* exceeded that for *NatTf* during the exponential phase. However, during the stationary phase the rate for *ConTf* was much lower than for *NatTf*. X-ray diffraction indicated the early production of elemental sulphur and reduced iron compounds in leach residues from *ConTf* limiting the rate. No evidence was found for direct attachment leaching. The order of oxidation of the minerals was pyrrhotite > sphalerite > chalcopyrite > violarite > pentlandite > pyrite because oxidation of Fe(II) to Fe(III) led to galvanic interactions where Fe(III) oxidises minerals with lower mixed-potential. Leaching models indicated a mixed kinetic regime with initial film diffusion control and subsequent shrinking-core product layer diffusion control.

Keywords: Bacteria; Bioleaching; Hydrometallurgy; Non-ferrous metallic ores; Sulphide ores

1. Introduction

The bacterial leaching of a copper–nickel–iron sulphide concentrate from Kambalda, Western Australia and a nickeliferous pyrrhotite concentrate from the Lynn Lake, Canada using *Thiobacillus ferrooxidans* was studied to attempt the possibility of preferentially leaching iron sulphides. Previous work on electrochemical leaching of pentlandite had indicated that in acidic sulphate media, considerable energy is necessary for pentlandite to react and its reaction rate is very slow but with ammonia the rate is much faster (Chileshe, 1994; Chileshe et al., 2000).

T. ferrooxidans is the dominant organism for oxidation of mineral sulphides at temperatures below 40 °C. Most *T. ferrooxidans* strains have optimum growth at 25–35 °C, but some Canadian strains show greater cold tolerance with an optimum temperature of 20 °C. The bacterium is found ubiquitously in nature and has a physiology ideally suited to growth in an inorganic mineral environment. It is autotrophic and obtains carbon for the synthesis of new cell material by fixation of carbon dioxide from the atmosphere. It derives its energy from oxidation-reduction reactions, where iron (II) or reduced sulphur compounds serve as the electron donor and oxygen is the preferred electron acceptor (Temple and Colmer, 1951; Rawlings and Woods, 1995), e.g reactions (1) and (2) below. Pyrite is a typical example of an energy source used by *T. ferrooxidans* (3).

$$2FeSO_4 + \tfrac{1}{2}O_2 + H_2SO_4 \rightarrow Fe_2(SO_4)_3 + H_2O \quad (1)$$

$$2S + 3O_2 + 2H_2O \rightarrow 2H_2SO_4 \quad (2)$$

$$FeS_2 + 3\tfrac{1}{2}O_2 + H_2O \rightarrow FeSO_4 + H_2SO_4 \quad (3)$$

In hydrometallurgical processes bacteria: (1) produce Fe(III), a strong oxidising agent for pyrite, and a common component of low-grade ores (2) produce H_2SO_4; and (3) dissociate the structure of pyrite. Biodegradation yields Fe^{2+} and S^{2-}, which can be used as energy sources by the bacteria to support growth. The organism's ability to grow autotrophically is a primary reason why this metal extraction process is economically competitive (Brierley, 1982). Below pH 4.5, microbial populations

☆ Presented at *Bio and Hydromet '02*, Cape Town, South Africa, March 2002.

* Corresponding author.
E-mail address: n.m.rice@leeds.ac.uk (N.M. Rice).

0892-6875/02/$ - see front matter © 2002 Published by Elsevier Science Ltd.
PII: S0892-6875(02)00118-8

that derive their energy from the oxidation of Fe^{2+} are more efficient than other agents supplying Fe(III) which is a key oxidising agent for degradation of most sulphide minerals and also microbial metabolism of Fe^{2+} generates heat energy which favours purely chemical reactions involving sulphides (Ehrlich and Brierley, 1990).

The large quantities of sulphuric acid produced make the environment in which *T. ferrooxidans* grows inhospitable to most other organisms. It is itself well adapted to high concentrations of sulphuric acid and grows optimally in the pH range 1.5–2.5 (Apel and Dugan, 1977). All *T. ferrooxidans* strains studied so far also fix nitrogen, i.e. are diazotrophic (Sugio et al., 1985), and can also grow in the absence of oxygen on reduced inorganic sulphur compounds using Fe(III) as an alternative electron acceptor (Drobner et al., 1990). Three strains were shown to be facultative hydrogen oxidisers (Barrett et al., 1993). The ability to oxidise hydrogen is repressed by iron (II) or sulphur and occurs only in the presence of oxygen.

Leaching mechanisms involving *T. ferrooxidans* include indirect leaching, direct leaching and galvanic conversion (Ehrlich and Brierley, 1990). For indirect leaching ferric sulphate, produced by reactions (1) and (3) acts as a strong oxidant for a variety of sulphide minerals (Dutrizac and MacDonald, 1974) even in the absence of oxygen or viable bacteria, e.g. for pentlandite.

$$NiFeS_{1.8} + 2Fe_2(SO_4)_3 \rightarrow NiSO_4 + 5FeSO_4 + 1.8S^0 \quad (4)$$

Ultimately, the indirect leaching mechanism depends upon biological regeneration of ferric sulphate via (1), elemental sulphur generated can be converted to sulphuric acid-reaction (2) which maintains the pH at favourable levels and also acts as a lixiviant.

Direct leaching without involvement of microbially produced ferric sulphate is inferred from observations of microbial attachment to metal sulphides but the best evidence comes from studies using synthetically prepared metal sulphide minerals free of iron. Incubation of washed cells with these synthetic substrates results in oxygen consumption and metal solubilisation. Because iron is nearly always available in natural leaching environments, both direct and indirect leaching mechanisms probably occur simultaneously.

Galvanic conversion involves physical contact between two dissimilar metal sulphide phases immersed in an electrolyte i.e. dilute sulphuric acid/ferric sulphate solution creating a galvanic cell resulting in rapid dissolution of the anodic mineral. *T. ferrooxidans* may accelerate the reaction by continuously oxidising any film of elemental sulphur that would otherwise form a product diffusion barrier.

The metal tolerance of *T. ferrooxidans* is important in mineral treatment especially the processing of concentrates (Tuovinen et al., 1971). The iron and sulphur oxidation mechanisms of *T. ferrooxidans* are generally insensitive to high concentrations of metals. Toxicity depends upon the physiological state of the bacteria and the oxidation states and speciation of the metals that govern their bioavailability. The toxic effects of metal ions are decreased as the complexity of the medium is increased (Ubaldini et al., 1997). Oxidation of Fe(II) is possible in the presence of Zn (0.15 M), Ni (0.17 M), Cu (0.16 M), Co (0.17 M), Mn (0.18 M) and Al (0.37 M), whereas U and anions of Se and Te are inhibitory at 0.8–3 mM/l. Molybdenum inhibits iron oxidation above 0.05 mM/l (Ng et al., 1997). Cr(VI) is toxic to both bacteria and humans. *T. ferrooxidans* has been shown to reduce Cr^{6+} to less soluble Cr^{3+} if elemental sulphur is the sole energy source for $[Cr^{6+}]$ as high as 2000 μM/l. Reduction is due to sulphite and thiosulphate generated during bacterial sulphur oxidation (Sisti et al., 1996). *T. ferrooxidans* is tolerant to Cd concentrations as high as 0.5 M (Baillet et al., 1997). Hg and Ag are toxic at below 0.5 μM/l. Other toxic metals include Au, Tl and Rb. Inhibitory levels of anions Cl^-, F^-, NO_3^- and CN^- have been reported (Hutchins et al., 1986).

2. Experimental

Two concentrates were used in this investigation: A nickel–copper–iron concentrate from Kambalda, Western Australia (Western Mining) and a nickeliferous pyrrhotite from Lyn Lake, Manitoba (Sherritt–Gordon Mines). These are subsequently referred to as ''Kambalda'' and ''Sherritt–Gordon'' respectively.

Experimental work was aimed at adapting *T. ferrooxidans* to growing on both the Kambalda and pyrrhotite concentrates at a pH of 2 and temperature of 30 °C. All experiments were performed using optimum conditions for the growth of *T. ferrooxidans* from the literature (Rossi, 1990). Pyrrhotite concentrate was used as substrate to attempt to 'acclimatise' the bacterium to a specific mineral species to try to achieve preferential leaching of pyrrhotite when this concentrate-grown strain (designated *ConTf*) was transferred to a culture containing Kambalda concentrate. All results were compared with control experiments using 2% W/V of thymol as bactericide (Meline et al., 1996) instead of a bacterial inoculum to distinguish between bacterial leaching and chemically controlled leaching.

pH measurement was made using a Jenway 3010 pH meter fitted with a resin-bodied saturated KCl electrode and temperature probe calibrated daily with fresh buffer solutions prepared weekly. The pH of the culture was adjusted to 2 using 5 mol/l sulphuric acid (Makamoto and Takahashi, 1995). To avoid contamination the pH electrode was washed in 98% ethanol and then dried

with sterile paper. The electrode was stored in 4 M KCl solution to prevent desiccation.

T. ferrooxidans (strain ATCC19859 from the National Collections of Industrial and Marine Bacteria, 1994) was cultured at 30 °C and pH 2 in 9 K medium (Silverman and Lundgren, 1959), omitting $FeSO_4$ as energy source. Although precipitation of jarosite and sulphates can occur in this culture medium it occurs very slowly and was considered unlikely to be a problem within the 7-day duration of most experiments so that the alternative of Norris and Kelly (1983) was not used. Parts A and B of the 9 K medium were made up separately and steam sterilised at 121 °C for 20 min in a pressure cooker. Sterilisation was ensured with autoclave tape, which turned from white to black once the required time, temperature and pressure were reached. Chemicals were Analar grade. Parts A and B of the 9 K medium were mixed at a 7:3 ratio and the pH adjusted to 2 using 5 mol/l sulphuric acid. During sterilisation of the $FeSO_4$ component some Fe(II) oxidised to Fe(III), resulting in a brown precipitate. Although literature states that loss of Fe(II) is not appreciable (Norris and Kelly, 1983) and that brown discolouration does not interfere with colony formation (Razzell and Trussell, 1963), it was preferred to filter through sterile 0.2 μm syringe filters to avoid this problem altogether.

All tests were carried out in duplicate in 250 ml Erlenmeyer flasks agitated in a reciprocating shaker bath incubator operating at 30 °C and 200 rpm. The flasks were sealed with a Whatman "Bugstopper™", i.e an autoclavable PTFE bung with a 0.2 μm filter that allows the passage of air but inhibited contaminating bacteria. The culture was monitored at regular intervals for contaminants using Gram's method for differential staining (see Mason, 2000 for details).

3. Cell growth and bacterial population measurement

Growth rate depends on the medium, genotype of the strain, temperature and the degree of aeration. As the density of the culture increases the rate of division decreases until the bacteria reach a concentration at which they no longer divide but are viable. Knowledge of the life cycle of *T. ferrooxidans* is important to ensure the reproducibility of leaching tests which should be performed with the bacterium in its log phase, i.e. actively growing and the birth-rate exceeding the death rate.

An attempt to measure bacterial population by optical density using a photometer (Maniatis et al., 1982) was unsuccessful so direct counting by microscope was used to estimate cell numbers. Other available methods based upon measurement of nitrogen or protein content or ammonia consumption were less convenient than counting. A Helber chamber with a light microscope (Maniatis et al., 1982) was used. Duplicate flasks of 9 K media were inoculated with revived bacteria. A culture aliquot was taken every 24 h, the bacterial cells dyed with methylene blue and counted.

The concentration of cells in the original culture per ml $= N \times (2 \times 10^7) \times$ dilution factor, where N is the average number of bacteria in the chamber (Fig. 1 shows the population growth curve for duplicate cultures) which allowed the optimum growth period for the bioleaching experiments to be estimated (Mason, 2000).

For microorganisms reproducing by binary fission a typical plot of logarithm (cell number) vs. incubation time shows four distinct phases (Prescott et al., 1990), viz. (i) lag phase; (ii) exponential (or log) phase; (iii) stationary phase; (iv) death phase. Fig. 1 follows this pattern. The exponential phase of bacterial growth started at day 3 and continued until day 16 when it reached the stationary phase. The Helber cell method does not distinguish between live and dead organisms, so it is not known when the death phase began but it was considered undesirable to enter this phase which is thus only of theoretical interest.

During the exponential phase, each microorganism is dividing at constant intervals. Thus, the population will double in number during a specific length of time called the generation time. As the population doubles every generation, the increase in population is always 2^n where n is the number of generations. The resulting population increase is exponential or logarithmic from which $n = (\log_{10} N_t - \log_{10} N_0)/\log_{10} 2$ where N_t is the number of cells at any time t. The *mean growth rate constant* (k), which is the number of generations per unit time (generations per hour) is

$$k = \frac{n}{t} = \frac{\log_{10} N_t - \log_{10} N_0}{0.301t}$$

and the mean generation time (g) is $g = 1/k$

From Fig. 1 g was estimated as 12 h for the period 3–5 days, i.e. 2 generations per day. On day 8 the population growth slowed to doubling every 6 days, hence

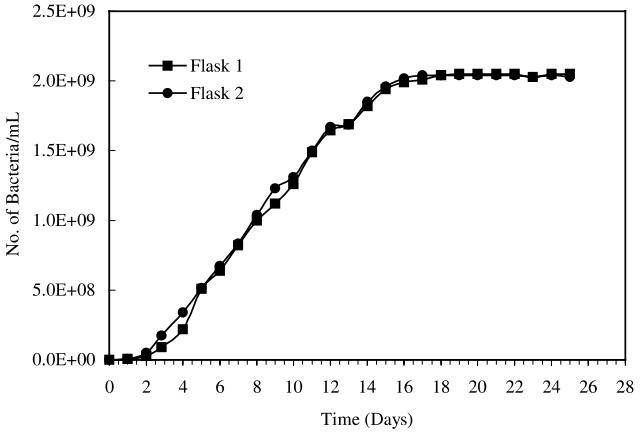

Fig. 1. Bacterial growth curve to calculate the mean generation time of *T. ferrooxidans*.

5-day-old cultures represent the optimum growth point. Therefore all bioleaching experiments were undertaken using a 5-day-old inoculum of *T. ferrooxidans.*

4. Characterisation of concentrates

Particle size distribution was determined with a Malvern Mastersizer Version 2.15 (Rawle, 1998). Fig. 2 shows both the % volume in size range and % undersize particle size distribution of the Kambalda concentrate.

The distribution is monomodal with a uniformity of 0.919 and slightly tails out at the finer particle sizes with $d_{0.5} = 60.3$ μm and 100% <563.7 μm. Particle size is important for the flash smelting of pentlandite and pyrrhotite, with particles larger than 100 μm difficult to smelt. The distribution was comparable to published data (Dunn et al., 1993).

The bacterial oxidation of various minerals by *T. ferrooxidans* has been reported for various particle size ranges from <10 to 200 μm (Schippers et al., 1996; Bhatti et al., 1993; Ohmura et al., 1993; Devasia et al., 1993). The optimum pulp density depends upon the size distribution. Smaller particle sizes require lower pulp densities as the greater the surface area the higher the risk of depletion of the number of bacteria in the initial stage. A system containing only surface-adsorbed bacteria would revert to lag phase growth and thus a lower solubilisation rate (Harvey and Crundwell, 1996). Since 68.8% of Kambalda concentrate was <100 μm, no further comminution was required.

Sherritt–Gordon concentrate displayed a bimodal distribution with uniformity 1.754. Visual inspection indicated that particle sizes >1 mm. were not present, so that the minor second peak of ~1000 μm is probably an artefact of the Mastersizer. $d_{(0.5)} = 32.5$ μm, with the $d_{(0.1)}$ and $d_{(0.9)} = 7.5$ and 122.0 μm respectively. 100% of the concentrate was below 563.7 μm.

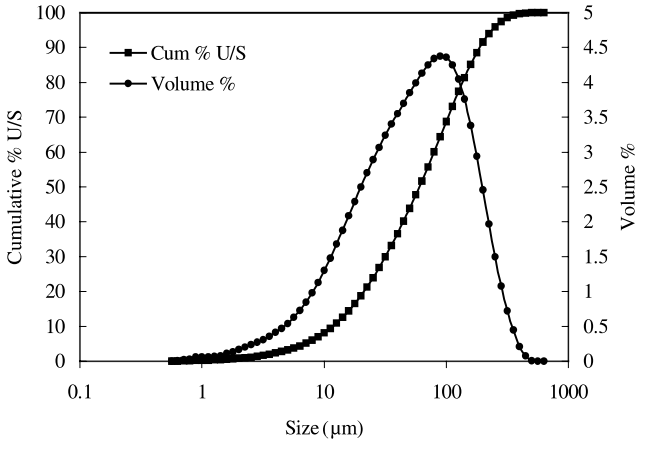

Fig. 2. Particle size distribution: Kambalda concentrate.

Powder X-ray diffraction (XRD) (APD1700 and a Philips model PW with CuK_α radiation) was used to identify solid leaching products from listed *d*-spacings for the principle minerals of nickel sulphide ores (ASTM index, 1962).

Most minerals associated with iron–nickel sulphide ores were present in Kambalda concentrate (Table 1). Pyrite and violarite were present along with a surprisingly large amount of sphalerite (18.1%). Galena was not observed due to lack of sensitivity, although evidence of its presence was found by microscopy and atomic absorption spectrophotometry (AAS). The gangue mineral was identified as chlorite, $(Mg,Fe)_5Al(AlSi_3)O_{10}(OH)_9$, an alteration product of biotite and hornblende.

An approximate mineral composition was estimated from the XRD data. Table 2 compares experimental results and published values (Dunn et al., 1993). Pentlandite, pyrite and violarite contents agreed well with but pyrrhotite differed from the literature value by 19.9% indicating that either the concentrate used was not representative or the use of a CuK_α radiation source masked the readings from the diffractometer slightly. As the other mineral contents agreed the problem may lie with the copper target. The only alternative would have been Mo or Co targets, both unavailable.

XRD results for Sherritt–Gordon concentrate are shown in Table 3. The trace was very simple compared

Table 1
XRD analysis of the Kambalda head sample

Peak number	% of concentrate	Incident/exit angle (θ)	*d*-spacing (Å)	Possible mineral species
1	3.85	12.3	7.196	Chlorite
2	12.09	28.8	3.100	Sphalerite
3	22.52	29.7	3.008	Pentlandite
4	3.30	30.2	2.959	Pyrrhotite
5	7.14	31.0	2.885	Violarite
6	4.40	33.2	2.698	Pyrrhotite
7	3.85	35.6	2.522	Chalcopyrite
8	4.67	37.3	2.411	Pyrite
9	4.40	44.3	2.045	Pyrrhotite
10	6.31	47.2	1.926	Pentlandite
11	6.04	47.6	1.910	Sphalerite
12	15.93	51.6	1.771	Pentlandite
13	5.50	56.8	1.621	Pyrite

Table 2
Mineral composition of Kambalda concentrate

Mineral	Weight percent	
	Literature (Dunn et al., 1993)	Experimental
Pentlandite	42	44.8
Pyrrhotite	32	12.1
Pyrite	6	10.2
Violarite	6	7.1

Table 3
XRD analysis of Sherritt–Gordon pyrrhotite concentrate

Mineral species	% of concentrate	Incident/exit angle (θ)	d-spacing (Å)
2° Pyrrhotite	23.5	30.1	2.969
3° Pyrrhotite	31.0	34.1	2.629
1° Pyrrhotite	45.5	21.5	2.053

to Kambalda concentrate. All three pyrrhotite peaks were very obvious and it was decided to study only depletion of this mineral during adaptation experiments.

4.1. Elemental analysis

Concentrate samples and leach residues were dissolved by treating 0.1 g in 12 ml aqua regia (HNO_3:HCl = 1:3) for 1 h. The resulting solutions were then filtered and made up to 100 ml with distilled water prior to analysis. Aqueous metal concentrations were determined by AAS using a Varian Techtron AA10 using the operating conditions in Table 4 (Varian-Techtron, 1989). Aqueous metal standards were 1000 mg/l (Spectrosol) diluted by volume to the required concentration using distilled water. All samples were diluted to the correct concentration range with distilled water and measured in triplicate. Samples with %RSD (random standard deviation) >1 were re-analysed immediately to eliminate the possibility of dilution by aspiration of distilled water between samples. Calibration lines were re-sloped using a mid-range standard every 10 samples to reduce 'drift' between calibrations. If a calibration line exhibited curvature, samples in the upper range were re-analysed after re-calibration or dilution. The 352.4 nm line was preferred to the more sensitive 232 nm line for Ni because the calibration is less curved over the working range and the signal is less susceptible to non-atomic absorbance, (Varian-Techtron, 1989; Gibson, 1996) and was the main line used for nickel.

Sulphur was analysed by barium sulphate precipitation after fusion with sodium carbonate and sodium peroxide. Silica was analysed by a colorimetry after digestion in hydrochloric acid (Hanusch, 2001).

Table 5 shows the averaged content of various elements in Kambalda concentrate with all results within 0.3%.

AAS confirmed the presence of galena (0.012% Pb) in the sample but the amount of zinc was only 0.36%, significantly lower than implied by XRD. This may be due to the scanning increments of the diffractometer. ($2\theta = 7°$ to 70° in increments of 5°.) Smaller increments would give more sensitive trace but increase scan time. Hence another mineral species might be masking the sphalerite peak and erroneously increasing its intensity. Magnesium confirms the presence of chlorite.

Table 6 shows AAS analysis of the nickel, iron and copper in Sherritt–Gordon concentrate to within 0.3%. Values for iron and copper are higher than Kambalda but nickel is lower as expected for a pyrrhotite concentrate.

4.2. Optical microscopy

Samples for optical microscopy were mounted in araldite and then ground and polished to a flat, mirrored surface. Polished sections were viewed under plane-polarised light and crossed polars with a Vickers 55 microscope at magnifications of X200, X300 and X400. The mineral species identified by XRD were confirmed including galena and sphalerite. A minor amount of anhedral galena with perfect cubic (1 0 0) cleavage visible as triangular pits was observed in amounts to corroborate the AAS result. Sphalerite was also present, although less than indicated by XRD. Pyrite occurred as highly metallic, brassy yellow grains throughout the polished section. Violarite was only visible at higher magnifications as brown-grey alteration product within grain boundaries and fractures of pentlandite.

Table 4
Operating conditions for metal analysis by AAS

Metal	Wavelength (nm)	Slit width (nm)	Range (mg/l)
Cobalt	240.7	0.2	0.05–15
Copper	217.9	0.2	0.2–60
Iron	372.0	0.2	1–100
Iron	386.0	0.2	1.5–200
Lead	217.0	1.0	0.1–30
Magnesium	202.6	1.0	0.15–20
Nickel	232.0	0.2	0.1–20
Nickel	352.0	0.5	1–100
Potassium	404.4	0.5	15–800
Sodium	330.2	0.5	2–400
Zinc	213.9	1.0	0.01–2

Table 6
Analysis of Sherritt–Gordon pyrrhotite concentrate

% Fe	% Ni	% Cu
39.9	3.08	0.73

Table 5
Elemental analysis of Kambalda concentrate

% Ni	% Cu	% Fe	% Co	% S	% SiO_2	% Pb	% Zn	% Mg	% K	% Na
13.75	1.05	35.97	0.24	27.79	6.14	0.012	0.359	2.02	0.048	0.00

4.3. Adaptation tests

For all test work, representative samples of the concentrates were prepared by coning and quartering. Subsamples were prepared using a Jones riffle (Wills, 1992). No further grinding was used as the particle size was in a suitable range for bacterial leaching.

Serial sub-culturing of selected strains in conditions of increasing amounts of substrate or heavy metals will produce a microbial strain having a higher oxidising ability for the given substrate or metal ion. Adaptation of *T. ferrooxidans* to Kambalda concentrate utilised a series of 7 day leaching tests in an acidic '9 K' medium (omitting $FeSO_4 \cdot 7H_2O$) at arbitrary standard conditions: Initial pH 2.0, 30 °C, Initial Substrate concentrations were: Ni 0.69, Fe 1.80, Cu 0.05 g/l.

One ml inoculum was transferred to 100 ml 9 K medium (Rossi, 1990). One g Kambalda concentrate was sterilised at 120 °C for 20 min and then added to the culture and the pH adjusted with sufficient 10 mol/l H_2SO_4 to initial pH 2.0. The amount of sulphuric acid for stabilising the pH at 2.0 for several hours was determined in a preliminary test and used subsequently. After sampling flasks were weighed and agitated, then re-weighed at fixed time intervals and initial weights restored by adding sterilised distilled water to compensate for evaporation. Every 24 h a 5 ml aliquot was taken after thorough mixing and decantation for analysis of Ni, Fe and Cu. After 7 days, the leach residue was filtered, washed with distilled water and ground in an agate pestle and mortar for XRD. Adaptation of the bacteria was achieved by a series of tests in which the inoculum of the nth test was a 1 ml sample taken from the suspension of the previous $(n-1)$th test during its late exponential phase. A sterile control flask containing 5 ml of methanol solution with 2% w/v thymol as a bactericide was run concurrently (Meline et al., 1996) to distinguish between bacterial and chemically controlled leaching. The pH of the medium ranged between 2.5 and 1.4 during tests. The strain of *T. ferrooxidans* adapted to the Kambalda concentrate was designated *NatTf.* After 18 weeks of adaptation, it was considered to be adapted to the concentrates. A strain similarly adapted to the pyrrhotite concentrate was designated *ConTf.*

5. Results and discussion

5.1. Adaptation of T. ferrooxidans to the Kambalda concentrate (strain NatTf)

Figs. 3–6 show the % metals extracted with increasing contact time for various adaptation tests. As expected, the % extraction for the control flask containing bactericide (Fig. 3) was much lower than observed for the biological leaching system even when using an unadapted strain of *T. ferrooxidans,* (Fig. 4), i.e. 10.6% Ni, 7.4% Fe and 3.8% Cu leached in 168 h compared to 20.2%, 11.5% and 5.8%. Fig. 5 shows that 1 week of adaptation increased the recovery of Ni and Cu further. After 18 weeks (Fig. 6) the extractions were 53.1% Ni,

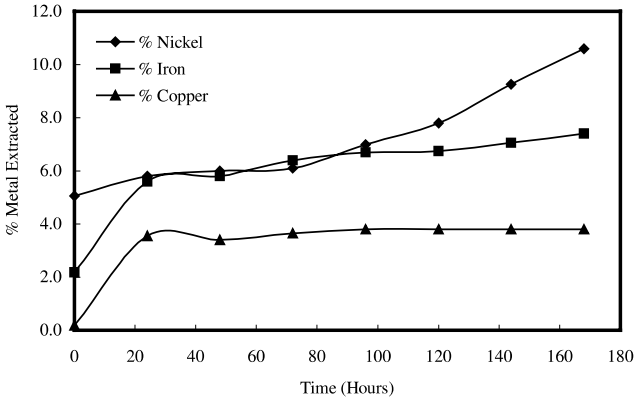

Fig. 3. % Metal extraction from Kambalda concentrate in control test using 2% w/v thymol as a germicide.

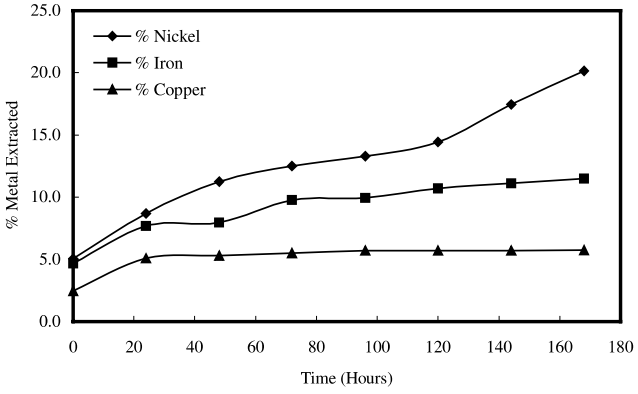

Fig. 4. % Metal extraction for unadapted *T. ferrooxidans* and Kambalda concentrate.

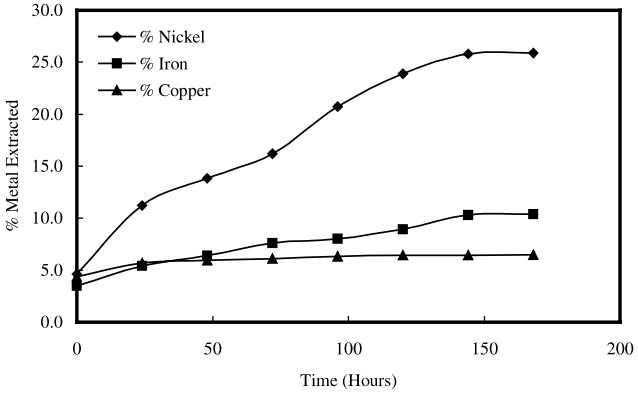

Fig. 5. % Metal extraction for *T. ferrooxidans* after one week of adaptation to Kambalda concentrate.

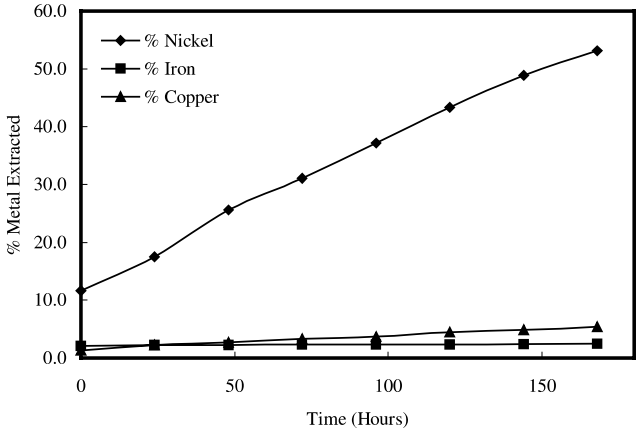

Fig. 6. % Metal extraction for *T. ferrooxidans* after 18 weeks of adaptation to Kambalda concentrate.

2.44% Fe and 5.39% Cu. Full data for each week of adaptation are available in Mason (2000).

As *T. ferrooxidans* became increasingly tolerant to the Kambalda concentrate the % Ni and Cu extraction increased whilst % Fe extraction decreased. The order of extraction for each week was initially Ni > Fe > Cu but this trend altered slightly after week 9 to Ni > Cu > Fe. Fig. 7 shows the final % metal extraction after 168 h leaching for each adaptation week over the whole period and the lines of best fit through the data points for each metal. The equations show that over 18 weeks Ni extraction increased by 1.99%, copper by 0.04% whilst the iron decreased by 0.56% per week on average.

A prolonged lag phase was observed for iron oxidation and gradually diminished as the bacteria became more adapted. There are two proposed explanations for this phenomenon (Rossi, 1990): (i) the time required to develop membrane-associated enzyme protecting systems which enable the cells to secure energy provision through ferrous iron oxidation. The protecting structure is thought to be metal specific and the length of the lag phase depend upon the specific metal cation, (ii) selection due to the time required for those bacterial cells that survived in the presence of the metal cation, to replace the bacterial population.

Table 7 gives solubilisation rates of the metals for control, unadapted and 18-week adaptation strains of *T. ferrooxidans* calculated from the gradient of the tangent to the exponential part of the curve. *T. ferrooxidans* more than doubled the solubilisation rate of Ni for an unadapted strain. After 18 weeks adaptation, the solubilisation rate of Ni increased to over eight times that for the control. That of Cu increased more slowly with values in control and unadapted experiments virtually identical. The solubilisation rate for Fe was greater for the unadapted strain compared to the control but decreased up to the 18th adaptation.

Hydrogen ions are important in the energy supply mechanism of *T. ferrooxidans* and the bacterial oxidation of ferrous iron and mineral sulphides involves electron transfer and movement of hydrogen ions. pH changed with time with the trend depending on adaptation week. Earlier adaptations showed an initial fall followed by a rise of about 0.2. Later adaptations showed a moderate increase in pH over the whole 7 days, from 2.0 to 2.3–2.4.

Fig. 8 shows % solubilisation of pentlandite after each week's adaptation calculated from the decrease in original peak intensity of the head sample XRD trace. It should be stressed that values calculated from XRD traces are only semi-quantitative. The amount of

Table 7
Solubilisation rates for the oxidation of Ni, Cu and Fe

Experiment	Solubilisation rate (mg/l/h)		
	Nickel	Iron	Copper
Control	0.213	0.4192	0.0073
Unadapted	0.546	0.655	0.0072
18th Adaptation	1.732	0.027	0.0124

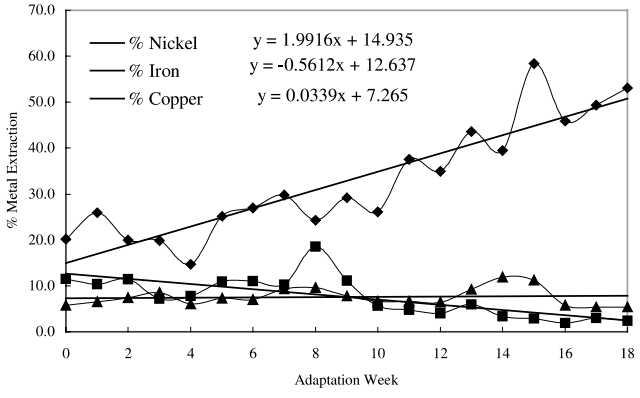

Fig. 7. % Extraction of Ni, Fe and Cu after each adaptation week for *T. ferrooxidans* after 168 h of leaching with linear trend lines.

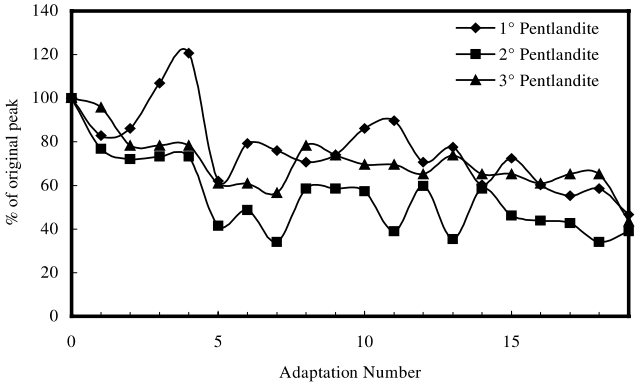

Fig. 8. % of original pentlandite XRD peaks *for each* adaptation week for Kambalda concentrate after 168 h of leaching using *T. ferrooxidans*.

mineral remaining in the leach residue was estimated for pentlandite, pyrrhotite, pyrite, chalcopyrite, violarite, sphalerite and chalcopyrite. Full data for all minerals and original XRD traces are given by Mason (2000).

Pyrrhotite was the first mineral completely solubilised. Both primary and secondary peaks were removed at weeks 13 and 15 respectively. The tertiary peak on the other hand, remained unchanged during all the experiments, which throws some doubt on its identification. The XRD equipment used was too insensitive to identify this peak. After week 14 the sphalerite secondary peak disappeared and only 5% of the tertiary peak remained at the end of the adaptation tests. Violarite was 60% depleted by the end of 18 weeks closely followed by pyrite, whose primary and tertiary peaks ended at 60% and 58% of their original levels. The primary and tertiary peaks of pentlandite were depleted by 40 and 50% respectively after 18 adaptations, with the secondary peak depleted by 70%. Chalcopyrite was the most resistant mineral to bacterial leaching, being 50% depleted by the end of the adaptations. The order of mineral solubilisation over one week appears to be: pyrrhotite > sphalerite > violarite > pyrite > pentlandite > chalcopyrite. Iron minerals are dissolving so the decreased dissolution of iron indicates that precipitation of insoluble compounds must be occurring during the test.

5.2. *Leaching using adapted* Thiobacillus ferrooxidans *(NatTf)*

Leaching experiments were performed using *NatTf T. ferrooxidans* strains from weeks 14 and 18 of adaptation. Week 14 was that which first oxidised 100% of the pyrrhotite. Week 18 was the most adapted to the concentrate. Fig. 9 shows % extraction of Ni, Cu and Fe over a period of five weeks for the latter. The pH rose from 1.95 to 2.45.

During the whole leaching process, *T. ferrooxidans* oxidised Fe(II) to Fe(III) according to the reaction,

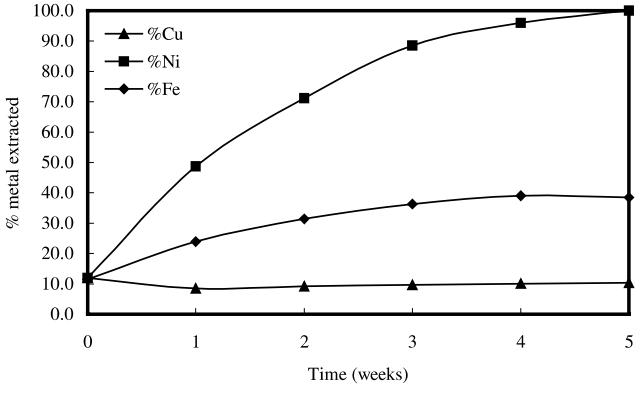

Fig. 9. % Metal extraction over five weeks using *T. ferrooxidans* (*NatTf* strain) after 18 weeks of adaptation to Kambalda concentrate.

$$4Fe^{2+} + O_2 + 4H^+ \rightarrow 4Fe^{3+} + 2H_2O \quad (5)$$

causing increased pH. The dissolution of most base metal sulphides occurs readily in the presence of ferric iron (Dutrizac and MacDonald, 1974) because of the redox potential (E_H) of the $[Fe^{3+}]/[Fe^{2+}]$ system (Sasaki et al., 1994, 1997), which is high enough to attack most mineral sulphides due to a galvanic couple effect where the mineral with lower mixed potential will be solubilised earlier than the other. It has been observed that mineral solubility generally increases in the presence of pyrite and a number of galvanic interactions have been reported (Berry et al., 1978). Table 8 shows an electrochemical series of metal sulphides in H_2SO_4 solution at pH 2.5 (Yakhontova, 1985).

Thus, ferric solutions have a high enough mixed potential to oxidise all of the minerals in Table 8 except pentlandite and pyrite. XRD indicates that pentlandite and pyrite were most resistant to oxidation. Pyrrhotite underwent complete oxidation within 5 weeks when using the 18 week adaptation, and only 16.7% of the secondary peak remained after 7 weeks of leaching with the 14 week adaptation. Pentlandite on the other hand, underwent a more complete solubilisation with the earlier adapted strain although this may be due to increased leaching time rather than any specific non-preferential leaching of pyrrhotite. For all other minerals, solubilisation was more pronounced for the longer adapted strain. Elemental sulphur, goethite and jarosite were observed in the leach residues. Sulphur is a by-product of the indirect leaching mechanism whilst secondary iron precipitates are characteristic of pyrrhotite oxidation. From the adaptation tests, the true order of mineral solubilisation is: pyrrhotite > sphalerite > chalcopyrite > violarite > pentlandite and Pyrite. With increasing adaptation, *T. ferrooxidans* was able to solubilise 100% nickel within 7 and 5 weeks for the 14 and 18-week adaptations respectively.

5.3. *Adaptation of* T. ferrooxidans *to the Sherritt–Gordon pyrrhotite concentrate (ConTf)*

T. ferrooxidans was successively sub-cultured in 100 ml of 9 K medium, containing 1 g of the pyrrhotite

Table 8
Electrochemical series of metal sulphides

Metal sulphide	Formula	Open-circuit potential vs. SHE (mV)
Galena	PbS	300
Chalcocite	Cu_2S	350
Sphalerite	ZnS	350
Chalcopyrite	$CuFeS_2$	400
Pyrrhotite	FeS	450
Pentlandite	(Fe, Ni)S	550
Pyrite	FeS_2	550–600

concentrate as energy source, to attempt to obtain a culture with a higher oxidising capacity for pyrrhotite for the Kambalda concentrate. *T. ferrooxidans* was adapted to the pyrrhotite concentrate using the technique described above. Data for each adaptation week are given by Mason (2000). Fig. 10 shows the results for adaptation week 16 and the full 16 weeks of adaptation are summarized in Fig. 11.

The extraction in the control experiment was generally lower than observed with the bacterium: 9.9% Ni, 23.0% Fe and 3.5% Cu were after 168 h compared with 9.9%, 26.6% and 7.9% for unadapted organisms. Results for Ni oxidation were identical, but *T. ferrooxidans* prefers pyrrhotite to $FeSO_4$ used as energy source in the control as indicated by increased iron oxidation. Cu also showed increased solubilisation for bacterial oxidation. After 16 weeks adaptation extraction was 19.5% Ni, 21.3% Fe and 9.9% Cu, an identical trend to Kambalda concentrate. The order of extraction for pyrrhotite was Fe > Ni > Cu, although, after week 10, Ni solubilisation initially overtook Fe until approximately 4 days leaching. From the lines of best fit the % Ni extraction

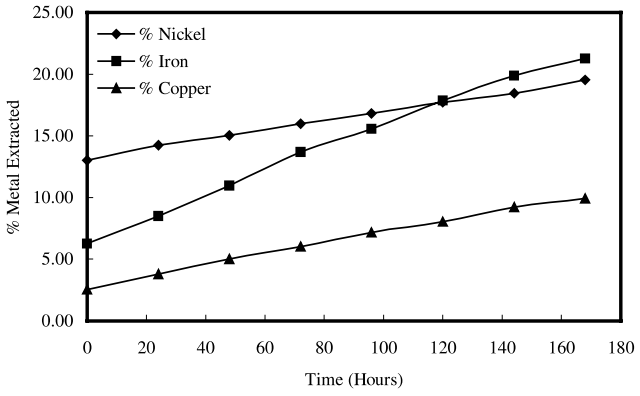

Fig. 10. % Metal extraction for *T. ferrooxidans* after 16 weeks of adaptation to Sherritt–Gordon concentrate (*ConTf* strain).

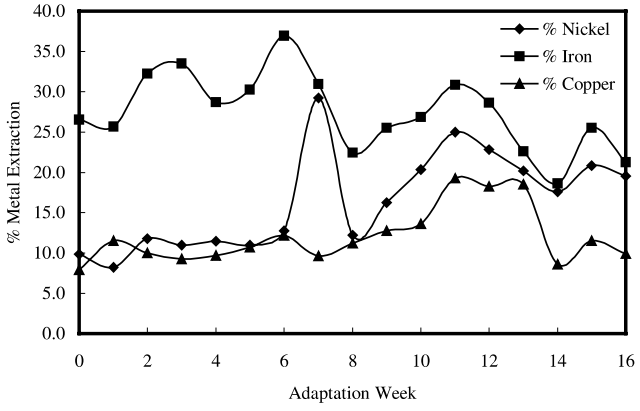

Fig. 11. % Extraction of Ni, Fe and Cu vs. adaptation week of *T. ferrooxidans* after 168 h of leaching of Sherritt–Gordon concentrate.

increased by 0.82 %, Cu by 0.30 % and Fe decreased by 0.50 % per week respectively over 16 weeks.

Table 9 gives solubilisation rates of Cu, Ni and Fe for control, unadapted and 16-week strains. The solubilisation rate of Ni doubles over 16 weeks. Control and unadapted tests gave similar rates for Cu and tripled by the 16th adaptation. The solubilisation rate of Cu in the pyrrhotite was three times that for the Kambalda concentrate whilst the rate for Ni was fifteen times slower for the pyrrhotite concentrate. The rate for iron increased from the control flask, to the unadapted strain but decreased at the end of the 16th adaptation.

5.4. Effect of pH

Initially pH increases and redox potential decreases (Bhatti et al., 1993; Ahonen et al., 1986) due to acid-consuming combination of non-oxidative and oxidative reactions

$$Fe_{1-x}S + 2H^+ \rightarrow (1-3x)Fe^{2+} + 2xFe^{3+} + H_2S \quad (6)$$

$$2Fe_{1-x}S + O_2 + 4H^+ \rightarrow (2-6x)Fe^{2+} + 4xFe^{3+} + 2S^0 + 2H_2O \quad (7)$$

This initial stage was almost identical in both control and inoculated systems, i.e. *T. ferrooxidans* has very little direct influence early in the process. The rate of chemical oxidation of Fe(II) increases with increasing pH, therefore this increase in pH probably represents the chemical oxidation of Fe(II) followed by Fe(III) iron hydrolysis resulting in a pH decrease to a level where *T. ferrooxidans* becomes active. After 48 h an acid-producing phase commenced due to a combination of sulphur (7) and Fe(II) oxidation and precipitation of basic iron compounds including ferrihydriite, goethite, jarosite and schwertmannite (8)–(11) and (12) (Bigham et al., 1992; Murad et al., 1994).

$$S^0 + 1\tfrac{1}{2}O_2 + H_2O \rightarrow SO_4^{2-} + 2H^+ \quad (8)$$

$$Fe^{3+} + 3H_2O \rightarrow Fe(OH)_3 + 3H^+ \quad (9)$$

$$Fe^{3+} + 2H_2O \rightarrow FeOOH + 3H^+ \quad (10)$$

$$X^+ + 3Fe^{3+} + 2SO_4^{2-} + 6H_2O \rightarrow XFe_3(SO_4)_2(OH)_6 + 6H^+, \quad \text{where } X = K^+, Na^+, NH_4^+ \text{ or } H_3O^+ \quad (11)$$

Table 9
Solubilisation rates for the oxidation of Ni, Cu and Fe for pyrrhotite concentrate

Experiment	Solubilisation rate (mg/l/h)		
	Nickel	Iron	Copper
Control	0.055	4.018	0.010
Unadapted	0.062	4.855	0.013
Week 16 *ConTf*	0.115	3.716	0.034

$$8Fe^{3+} + SO_4^{2-} + 14H_2O \rightarrow Fe_8O_8(OH)_6SO_4 + 22H^+ \quad (12)$$

No such compounds were detected in the short period of the adaptation tests.

5.5. Mineral solubilisation

Fig. 12 illustrates the % solubilisation of pyrrhotite after each adaptation week calculated by XRD. Only pyrrhotite was estimated. After 7 days leaching in the sterile control, the pyrrhotite content was lower, indicating its susceptibility to chemical dissolution. Fig. 12 indicates that the strong d_{228} pyrrhotite doublet centred at 2.05 Å underwent 50% dissolution in 7 days for the 16 weeks strain. This agrees with Bhatti et al. (1993) who found that pyrrhotite underwent complete dissolution after 14 days with *T. ferrooxidans*.

Elemental sulphur was evident in all residues except the control, implying an indirect mechanism where the initial chemical step consumes acid and produces sulphur followed by bacterial acid production and oxidation of sulphur and iron.

5.6. Treatment of Kambalda concentrate with the ConTf Strain

Strains of *ConTf* chosen after 9 and 16 weeks adaptation to pyrrhotite concentrate were used to assess the time required for *T. ferrooxidans* to solubilise 100% of the nickel contained within the Kambalda concentrate and to identify any secondary iron mineral formation. Metal extraction is shown in Fig. 13 for the 16-week adapted strain. Full data are in Mason (2000). The general metal solubilisation order was again Ni > Fe > Cu.

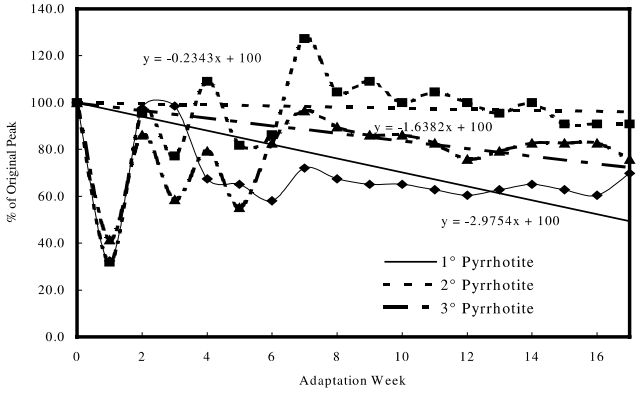

Fig. 12. % of original pyrrhotite XRD peak vs. adaptation week after 168 h of leaching using *T. ferrooxidans* (linear trendlines, Sherritt–Gordon concentrate).

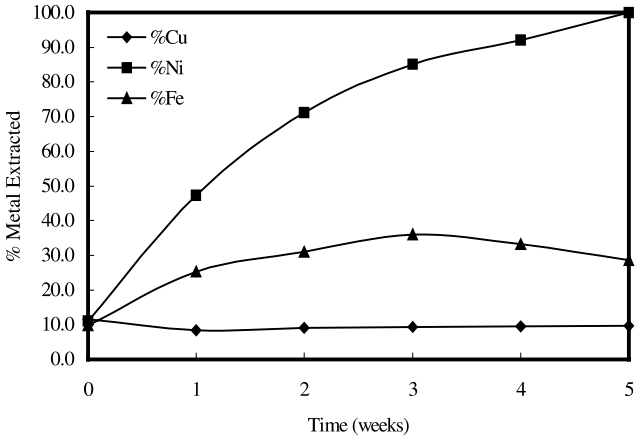

Fig. 13. % Metal extraction over five weeks from Kambalda concentrate using a 16 week adapted *ConTf* strain of *T. ferrooxidans*.

The curves correspond closely to population growth curves (Fig. 1). An initial rapid solubilisation was observed for the first 7 days of leaching corresponding to the log growth phase and then a decrease in solubilisation rate indicates the start of the stationary phase. Table 10 gives solubilisation rates for Ni, Cu and Fe for the exponential and stationary periods of growth.

A distinct change in solubilisation rate was observed between both the adaptation weeks and the growth phases. The main difference between the 9th and 16th week adaptations was for the rate of iron solubilisation. During the stationary phase of bacterial growth, the Fe solubilisation rate was reduced. For the 16-week adaptation strain, Fe solubilisation was negative indicating precipitation from solution. This was confirmed by the presence of an ochre precipitate appearing after one week of leaching and subsequent XRD confirmed this as an Fe hydroxide.

The results for Ni indicate a greater solubilisation rate for the earlier adaptation rather than the later in the initial stages. During the stationary phase, this reversed,

Table 10
Solubilisation rates for the oxidation of nickel, copper and iron from Kambalda concentrate using *ConTf* strain of *T. ferrooxidans*

Adaptation	Solubilisation rate (mg/l/h)					
	Exponential phase			Stationary phase		
	Nickel	Iron	Copper	Nickel	Iron	Copper
9th week	1.7	0.91	0.02	0.31	0.25	-1.0×10^{-2}
16th week	1.49	1.67	-1.1×10^{-3}	0.38	−0.10	6.0×10^{-4}

Table 11
Solubilisation rates for the oxidation of Kambalda concentrate using *NatTf* strains

Adaptation	Solubilisation rate (mg/l/h)					
	Exponential phase			Stationary phase		
	Nickel	Iron	Copper	Nickel	Iron	Copper
12th Week	0.88	0.13	0.0137	0.51	0.10	4.0×10^{-3}
18th Week	1.51	1.33	−0.0107	0.39	0.26	1.2×10^{-3}

and the later strain exhibited a slightly greater Ni solubilisation rate. The rate of Cu solubilisation was low for both adaptations, and decreased even further in the stationary phase.

Table 11 shows the metal solubilisation rates for the *NatTf* strain as a comparison.

The main difference between the *NatTf* and *ConTf* strains would seem to be the solubilisation rate during the exponential phase of bacterial growth. The rate for the *ConTf* strain is far greater than that of the *NatTf* strain for Cu, Ni and Fe during this phase, however, the rate for *ConTf* strain drops sharply during the stationary phase compared to *NatTf*. This may be due to the earlier accumulation of secondary iron precipitates observed, which would coat the mineral surfaces inhibiting the rate of further solubilisation. The time taken for 100% solubilisation of Ni decreases with increasing adaptation of *T. ferrooxidans* to pyrrhotite concentrate, when grown on Kambalda concentrate.

XRD traces for the leach residue of Kambalda concentrate using *ConTf* showed that, pyrrhotite, chalcopyrite and sphalerite are completely solubilised for both adaptations. For all other minerals, oxidation increased for the later adaptation and the order of solubilisation was the same as for *NatTf*.

5.7. Precipitation of iron

The bio-oxidation of pyrrhotite increases pH, causing formation of a variety of iron precipitates including jarosite, ferrihydrite, goethite and schwertmannite. During leaching of Kambalda concentrate using both strains, the leach residues were observed to be an ochreous colour. Jarosite was detected by an XRD doublet at 3.11 Å (0.311 nm) with a goethite peak at 2.690 Å (0.269 nm). Schwertmannite (Bhatti et al., 1993) could not be detected owing to its very poor crystallinity and the masking effect of other, better-ordered minerals.

5.8. Reaction kinetics

Leaching kinetics are controlled either by diffusional mass transfer of either reactant or product ions through a liquid boundary layer or a product metal deposit (Levenspiel, 1999). Liquid film diffusion control would be implied by linear first order kinetics, i.e a plot of α, the fraction of Ni solubilised, vs. time should be linear. If product layer diffusion controls rate, then α vs. $t^{1/2}$ or α^2 vs. t should be linear. Strict application of shrinking core model theory indicates that for boundary layer control,

$$kt = 1 - 0.667\alpha - (1-\alpha)^{\frac{2}{3}} \tag{13}$$

is linear for a given particle size range. Chemical reaction rate control gives

$$kt = 1 - (1-\alpha)^{\frac{1}{3}} \tag{14}$$

as a linear plot of gradient k (the first-order rate constant for the surface reaction). Since the progress of the reaction would be unaffected by the presence of any product layer; the quantity of material reacting is proportional to the available surface of unreacted core. When no product layer forms, the reacting particle shrinks during reaction, finally disappearing. For small particles, this is governed by a Stokes regime, for which,

$$kt = 1 - (1-\alpha)^{\frac{2}{3}} \tag{15}$$

The applicability of each kinetic model was assessed using nickel-leaching data from Fig. 9. Results for each model are plotted in Figs. 14–16. Equations for the lines of best fit are given in Table 12 for each model with the respective correlation coefficients. Also included is the equation and correlation coefficient for Fig. 9, which is an α vs. time plot.

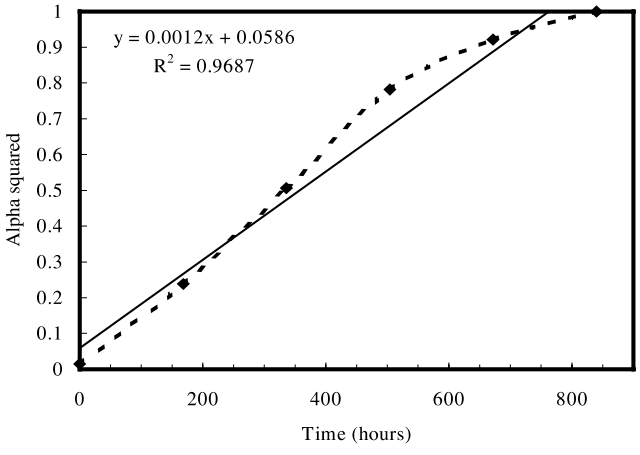

Fig. 14. Parabolic product layer diffusion model of leaching kinetics of nickel from Fig. 9.

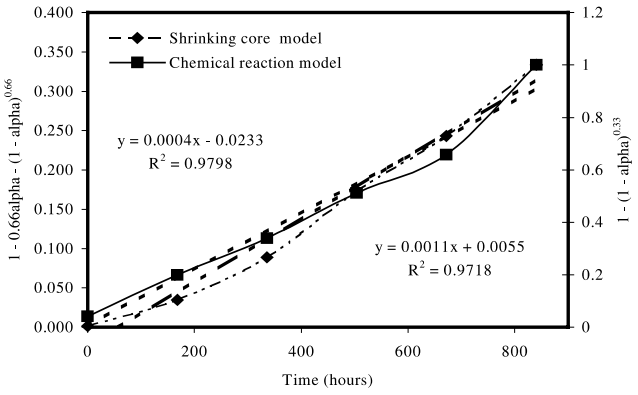

Fig. 15. Shrinking core and chemical reaction models of leaching kinetics of nickel from Fig. 9.

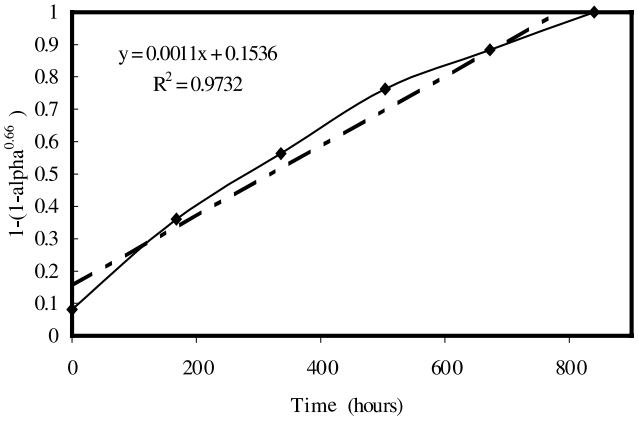

Fig. 16. Shrinking sphere model, Stokes' regime for leaching kinetics of nickel from Fig. 9.

Equations for the lines of best-fit and respective correlation factors for other leaching experiments are given in Mason (2000). They show increased correlation coefficients with increasing bacterial adaptation to Kambalda concentrate, until R^2 reached 0.9957 for the 18th week. Correlation coefficients for the leaching tests over a period of several weeks were lower than for 1-week adaptation tests. This seems to indicate preference towards liquid film diffusion kinetics during the first week turning into some other regime during the following weeks.

Table 12 indicates that the shrinking core model approaches linearity more closely than the others; i.e that the resistance to diffusion through a product layer controls the rate of reaction of the bacterial leaching of Kambalda concentrate. This may be attributed to the formation of a sulphur layer, as detected by XRD during the longer leaching tests, and would thus slow down the rate of reaction.

6. Conclusions

T. ferrooxidans was successfully adapted over 18 weeks to leaching of a copper–nickel–iron sulphide concentrate from Kambalda, Western Australia (strain *NatTf*). *T. ferrooxidans* increased the solubilisation of metal above that obtained using a chemical system only. The order of solubilisation of the minerals was pyrrhotite > sphalerite > chalcopyrite > violarite > pentlandite and pyrite. The bacterium was also adapted a pyrrhotite concentrate from Lynn Lake Manitoba, (strain *ConTf*). *T. ferrooxidans* increased nickel and copper solubilisation but extraction of iron decreased over 16 weeks of adaptation. The solubilisation rate of iron increased considerably compared to *NatTf*. The nickel solubilisation rate was slower but the copper leaching rate tripled. After the sixteenth adaptation week, pyrrhotite dissolved completely over 7 days.

Leaching of Kambalda concentrate with both strains gave 100% nickel solubilisation in 5 weeks. The extraction curves corresponded closely to the population growth curve of *T. ferrooxidans*. The rate for *ConTf* was greater than *NatTf* during the exponential phase of growth, with the opposite true for the stationary phase. The sharp decline of solubilisation rate for *ConTf* is thought to be due to earlier accumulation of iron minerals and elemental sulphur coating the mineral surface during leaching.

The objective of adapting the bacterium to the preferential leaching of pyrrhotite over pentlandite was not successful. *T. ferrooxidans* can be adapted to leaching of a nickel–iron concentrate with preferential leaching of nickel over iron and copper but it was not possible to upgrade the material by preferential leaching of pyrrhotite.

No evidence was found for the direct mechanism of leaching with *T. ferrooxidans*.

Leaching kinetics were controlled by a mixed kinetic regime for the final adaptation with the *NatTf* with film

Table 12
Lines of best-fit equations and correlation factors for various kinetic leaching models

Kinetic model	Figure no.	Line of best fit	Correlation factor
Shrinking core model	15	$y = 0.0004x - 0.0233$	0.9798
Chemical reaction model	15	$y = 0.0011x + 0.0055$	0.9718
Shrinking sphere, Stokes regime	16	$y = 0.0011x + 0.1536$	0.9732
Product layer diffusion, parabolic	14	$y = 0.0012x + 0.0586$	0.9687
Liquid film diffusion	9	$y = 17.129x + 26.549$	0.8943

diffusion control for the first week of leaching, followed by kinetics that most closely matched the shrinking core regime for the remaining weeks due to a product layer of sulphur and reduced iron compounds.

This study could be supplemented by the following further experimental work:

Use of other species such as the *Sulpholobus* genus able to grow in temperatures in excess of 60 °C.

Use of a mixed bacterial culture with a species such as *T. thiooxidans* to oxidise the rate-determining sulphur layer on the surface of the mineral. This would be especially useful for *ConTf* strain whose reaction rate during the stationary phase was severely reduced by product layer effects.

A more thorough investigation into kinetic models of metal extraction.

Application of electrochemical techniques (Luo, 1990; Chileshe, 1994) including potentiometry, cyclic voltammetry, chronoamperometry and chronopotentiometry.

Acknowledgements

The authors wish to thank the EPSRC, U.K., for the provision of a scholarship for Lisa Mason. Thanks are due to Western Mining Limited, Australia and to Sherritt–Gordon Mines Ltd., Canada for provision of the concentrates used and also to David Dean, Simon Lloyd and Robert Willan for their very helpful technical assistance with various practical aspects of the investigation.

References

ASTM Index, Index to the X-ray Powder Data File, 1962. ASTM Special Technical Publication 48-4. ASTM, Philadelphia, PA, USA, pp. 329–368.

Ahonen, L., Hiltunen, P., Tuovinen, O.H., 1986. The role of pyrrhotite and pyrite in the bacterial leaching of chalcopyrite. In: Lawrence, R.W., Branion, R.M.R., Ebner, H.G. (Eds.), Fundamental and Applied Biohydrometallurgy. Elsevier, Amsterdam, pp. 13–22.

Apel, W.A., Dugan, P.R., 1977. Hydrogen ion utilisation by iron-grown *Thiobacillus ferrooxidans*. In: Murr, L.E., Torma, A.E., Brierley, J.A. (Eds.), Metallurgical Applications of Bacterial Leaching and Related Microbiological Phenomena. Academic Press, New York, NY, pp. 45–59.

Baillet, F., Magnin, J.P., Cheruy, A., Ozil, P., 1997. Cadmium tolerance and uptake by a *Thiobacillus ferrooxidans* biomass. Environmental Technology 18, 631–638.

Barrett, J., Hughes, M.N., Karavaiko, G.I., Spencer, P.A., 1993. In: Metal Extraction by Bacterial Oxidation of Minerals. Ellis Horwood, London, UK, pp. 63–64.

Berry, B.K., Murr, L.E., Hiskey, J.B., 1978. Galvanic interaction between chalcopyrite and pyrite during bacterial leaching of low-grade waste. Hydrometallurgy 3, 309–326.

Bhatti, T.M., Bigham, J.M., Carlson, L., Tuovinen, O.H., 1993. Mineral products of pyrrhotite oxidation by *Thiobacillus ferrooxidans*. Applied and Environmental Microbiology 59, 1984–1990.

Bigham, J.M., Schwertmann, U., Carlson, L., 1992. Mineralogy of precipitates formed by the biogeochemical oxidation of Fe(II) in mine drainage. In: Skinner, H.C.W., Fitzpatrick, R.W. (Eds.), Biomineralisation Processes of Iron and Manganese. Catena Verlag, Hamburg, Germany, pp. 219–232.

Brierley, C.L., 1982. Microbiological mining. Scientific American 247 (2), 42–51.

Chileshe, F., 1994. An electrochemical study of the oxidative dissolution of synthetic nickel–iron–sulphide minerals in aqueous media. M.Sc. (Eng) thesis, University of Leeds, UK.

Chileshe, F., Rice, N.M., Taylor, N., 2000. An electrochemical study of the oxidative dissolution of synthetic nickel–iron sulphides. In: Wills, B.A. (Ed.), Commercial Aqueous Media. Proc. Hydrometallurgy 2000, Adelaide, Australia. Minerals Engineering International, Falmouth, pp. 25–26.

Devasia, P., Natarajan, K.A., Sathyanarayana, D.N., Ramananda Rao, G., 1993. Surface chemistry of *Thiobacillus ferrooxidans* relevant to adhesion on mineral surfaces. Applied and Environmental Microbiology 59, 4051–4055.

Drobner, E., Huber, H., Stetter, K.O., 1990. *Thiobacillus ferrooxidans*, a facultative hydrogen oxidiser. Applied and Environmental Microbiology 56, 2922–2923.

Dunn, J.G., Mackey, L.C., Smith, T.N., Stevenson, I.R., 1993. Mineralogical study of products collected following pilot-scale smelting of some Western Australian nickel sulphide concentrates, Transactions of the Institution of Mining and Metallurgy, Section: Mineral Processing and Extractive Metallurgy 102, pp. C75–C82.

Dutrizac, J.E., MacDonald, R.J.C., 1974. Ferric iron as a leaching medium. Minerals Science and Engineering 6 (2), 59–100.

Ehrlich, H.L., Brierley, C.L., 1990. In: Ehrlich, H.L., Brierley, C.L. (Eds.), Microbial Mineral Recovery. McGraw-Hill, New York, NY, pp. 55–73.

Gibson, R.W., 1996. The hydrometallurgical recovery of nickel from laterite ores by a chloride route using the proprietary metal extractants Cyanex 301 and 302. Ph.D. thesis, University of Leeds, UK.

Hanusch, A., 2001. Mineral and metallurgical laboratory techniques. Mineral Analysis Laboratory Manual. Department of Mining and Mineral Engineering, University of Leeds, pp. 8, 10–11.

Harvey, P.I., Crundwell, F.K., 1996. The effect of As (III) on the growth of *Thiobacillus ferrooxidans* in an electrolytic cell under controlled redox potentials. Minerals Engineering 9 (10), 1059–1068.

Hutchins, S.R., Davidson, M.S., Brierley, J.A., Brierley, C.L., 1986. Microorganisms in reclamation of metals. Annual Review of Microbiology 40, 311–336.

Levenspiel, O., 1999. In: Chemical Reaction Engineering, third ed. J. Wiley and Sons, Chichester, UK, pp. 566–588.

Luo, R., 1990. An electrochemical study of the oxidative dissolution of synthetic copper–silver–selenide minerals in aqueous media, Ph.D. thesis, University of Leeds, UK.

Makamoto, T.K., Takahashi, N.T., 1995. Adaptation of *Thiobacillus ferrooxidans* to nickel ion and bacterial oxidation of nickel sulphide. Biotechnology Letters 17 (2), 229–232.

Maniatis, T., Fritsch, E.F., Sambrook, J., 1982. Molecular cloning—a laboratory manual, 1982. Cold Spring Harbor Laboratories. Cold Spring Harbour, New York, pp. 58–61.

Mason, L.J, 2000. The adaptation of *Thiobacillus ferrooxidans* for the treatment of a nickel–iron sulphide ore, Ph.D. Thesis, University of Leeds, UK.

Meline, F., Mustin, C., de Donato, P., 1996. Inhibition de l'oxydation bactérienne de la pyrite par adsorption de Thymol, Comptes Rendus Academe Sciences, Paris, Sciences de la terre et desplanètes, 322 (IIa), pp. 959–964.

Murad, E., Schwertmann, U., Bigham, J.M., Carlson, L., 1994. The mineralogical characteristics of poorly crystalline precipitates formed by oxidation of Fe^{2+} in acid sulphate waters. In: Alpers,

C.N., Blowes, D.W. (Eds.), Environmental Geochemistry of Sulphide Oxidation. American Chemical Society, NY, USA.

National Collections of Industrial and Marine Bacteria, 1994. Catalogue of Strains, Aberdeen, Scotland, 205.

Ng, K.Y., Oshima, M., Blake, R.C., Sugio, T., 1997. Isolation and some properties of an iron-oxidising bacterium *Thiobacillus ferrooxidans* resistant to molybdenum ion. Bioscience Biotechnology and Biochemistry 61 (9), 1523–1526.

Norris, P.R., Kelly, D.P., 1983. Iron and mineral oxidation with *Leptospirillum*-like Bacteria. In: Rossi, G., Torma, A.E. (Eds.), Recent Progress in Biohydrometallurgy. McGraw-Hill, NY, USA, p. 83.

Ohmura, N., Kitamura, K., Saiki, H., 1993. Selective adhesion of *Thiobacillus ferrooxidans* to pyrite. Applied and Environmental Microbiology, 4044–4050.

Prescott, L.M., Harley, J.P., Klein, D.A., 1990. Microbiology, 111–117.

Rawle, A., 1998. Basic principles of particle size analysis. Malvern Instruments Ltd, www.malvern.co.uk, pp. 8.

Rawlings, D.E., Woods, D.R., 1995. Development of improved biomining bacteria. In: Gaylarde, C.C., Videla, H.A. (Eds.), Bioextraction and Biodeteriation of Metals. Cambridge University Press, Cambridge, U.K, pp. 63–84.

Razzell, W.E., Trussell, P.C., 1963. Isolation and properties of an iron-oxidising *Thiobacillus*. Journal of Bacteriology 85, 595–603.

Rossi, G., 1990. In: Biohydrometallurgy. McGraw-Hill, London, UK, pp. 137–142.

Sasaki, K., 1997. Raman study of the microbially mediated dissolution of pyrite by *T. ferrooxidans*. The Canadian Mineralogist 35, 999–1008.

Sasaki, K., Konno, H., Inagaki, M., 1994. Structural strain in pyrite evaluated by powder X-ray diffraction. Journal of Materials Science 29, 1666–1669.

Schippers, A., Jozsa, P., Sand, W., 1996. Sulphur chemistry in bacterial leaching of pyrite. Applied and Environmental Microbiology, 3424–3431.

Silverman, M.P., Lundgren, D.G., 1959. Studies on the chemoautotrophic iron bacterium Ferrobacillus ferrooxidans. I. An Improved Medium and a Harvesting Procedure for Securing High Cell Yields. Journal of Bacteriology 77, 642–647.

Sisti, F., Allegretti, P., Donati, E., 1996. Reduction of Dichromate by *Thiobacillus ferrooxidans*. Biotechnology Letters 18 (12), 1477–1480.

Sugio, T., Domatsu, C., Munakata, O., Tano, T., Imai, K., 1985. Role of Ferric Iron Reducing System in Sulphur Oxidation of *Thiobacillus ferrooxidans*. Applied and Environmental Microbiology 49, 1401–1406.

Temple, K.L., Colmer, A.R., 1951. The Autotrophic Oxidation of Iron by a New Bacterium: *Thiobacillus ferrooxidans*. Journal of Bacteriology 62, 605–611.

Tuovinen, O.H., Niemela, S.I., Gillenberg, H.G., 1971. Tolerance of *Thiobacillus ferrooxidans* to some metals. Antonie van Leeuwenhoek. Journal of Microbiological Serology 37, 489–496.

Ubaldini, S., Veglió, F., Toro, L., Abbruzzese, C., 1997. Biooxidation of arsenopyrite to improve gold cyanidation: study of some parameters and comparison with grinding. International Journal of Mineral Processing 52, 65–80.

Varian Techtron Pty. Ltd., 1989. Flame Absorption Spectrophotometry Analytical Methods. Victoria, Australia.

Wills, B.A., 1992. In: Mineral Processing Technology, sixth ed. Pergamon Press, Oxford, pp. 89–90.

Yakhontova, L.K., 1985. The role of the sulphide constitution in the process of their bacterial leaching. In: Karavaiko, G.I., Groudev, S.N. (Eds.), Biogeotechnology of Metals. UNEP Centre of International Projects, Moscow, USSR, p. 216.